SUPPLEMENTAL MATERIAL

Michalowski and Little – "Role of *cis*-acting sites in stimulation of the phage λ P_{RM} promoter by CI-mediated looping"

A. Plasmids

A.1. Plasmids with *lacO* / P_L

pJWL334 (1) was used as cloning vector for most plasmids used in phage-by-plasmid crosses. It carries a multiple cloning site followed by a strong *trp a* terminator. We found that plasmids carrying the O_L region cloned into the multiple cloning site must be maintained in a host making CI (or Lac repressor in the case of pJWL808), presumably because high-level expression of P_L is toxic, despite the presence of the *trp a* terminator downstream of P_L. In contrast, plasmids with P_R oriented towards *trp a*, such as pJWL631, do not require presence of CI for maintenance.

pJWL808 -- this was made in several steps (not described), and used (but not named) in (2). It contains λ DNA (3) from λ nucleotides 35285 (early in the ***N*** gene) to 35939 (late in the *rexB* gene); λ residues 35555-35586 are replaced with the sequence GCATGCAATTGTGAGCGGATAACAATTCGTT, which includes *lacO* (underlined). This segment is cloned into pJWL334, with P_L oriented towards *trp a*.

A.2. Plasmids used for construction of phages altered in the O_L region

pJWL1293 -- this plasmid carries the wild-type O_L region DNA from positions 35357 to 35872. It was isolated by PCR using primers bamrexb and oLKpn with λJL163 as template, digestion with BamHI and KpnI, ligation into pJWL334 cut with the same enzymes, and transformation into strain JL9058. P_L is oriented towards *trp a*; pJWL1293, pJWL1294 and pJWL1295 (see below) were maintained in a host producing CI. pJWL1293 was used as an O_L^+ control in phage-by-plasmid crosses (section B.2) with λJL481 and λJL483.

pJWL1294 – Site-directed mutagenesis (SDM) was done as described (4), using primers IHF80for and 79mutrev and pJWL1293 as template, introducing the *IHFmut* mutation.

pJWL1295 -- as pJWL1294, using primers 105for and 85rev, introducing the *ΔUP* mutation.

A.3. Plasmids used for construction of reporters with changes in the O_L region

Plasmids were made with variants of the O_L region located distal to *lacZ* (Fig. S1 in (5)). These were derived from pJWL1157 and pJWL1158 (Table S1), which include the wild-type O_L

region and its O_L3-4 derivative, respectively. Primers for SDM and resulting genotypes are listed in Table S2. Presence of the desired sequence was verified by DNA sequencing.

A. 4. Other plasmids

pJWL521: This was made in several steps (not described). It carries a promoterless, truncated *c*I gene from residues ~37925 to 37459 (amino acids 5 to 160) and the *c*I857 allele (A66T).

B. Phage Strains

B.1. Selection for phages with altered O_L regions--approach

We developed a selection for phage recombinants, arising from phage-by-plasmid crosses, that carry the plasmid-borne O_L region (Fig. S2). This selection should be of general use for this purpose. The parental phage (section B.1.a. below) carries a *lac* operator located just after the start of P_L (2), in the same location, at +5 to +25 relative to the P_L start site, as in the natural *lac* promoter. On strain JL6142, with no Lac repressor, this phage forms turbid plaques resembling those of wild-type λ. The *lacO* / P_L phage cannot grow in the presence of Lac repressor, affording a selection for recombinants that had lost the *lacO* allele, termed $LacI^R$. In the crosses described here, the desired recombinants exhibited an altered plaque morphology, but this feature is not required for the isolation of O_L variants, since DNA sequencing of $LacI^R$ recombinants provides a secondary screen for the genotype.

The *lacO* / P_L phages with P_{RM}^+ or *prm240* were crossed with plasmids carrying the O_L region with *IHFmut* or *ΔUP*, and cross progeny were plated on strain JL7937, which produces a high level of Lac repressor. In crosses with a control O_L^+ plasmid, the resulting $LacI^R$ plaques, which should be genetically wild-type, were of uniform morphology, with the same appearance as plaques of wild-type λ. $LacI^R$ phages produced in crosses with the *IHFmut* and *ΔUP* plasmids yielded a mixture of plaque morphologies. When the parental phage was P_{RM}^+, about 1/3 of the plaques resembled wild-type, while about 2/3 were about the same size but somewhat less turbid than the wild-type When the parental phage was *prm240*, recombinants made nearly clear plaques. The less-turbid plaque-formers were found by DNA sequencing to carry the *IHFmut* or *ΔUP* alleles.

B.1.a. Phages with *lacO* / P_L

λJL489 -- λJL537 *v2 v1 v3* was crossed with pJWL808 in strain JL7209. Non-virulent phage recombinants, which had lost the O_L1 allele *v2* by recombination with the plasmid, were

identified by plating on a mixed indicator, consisting of JL2497 and JL5895, as described (5) and screening for turbid plaques. The top agar contained 0.2 ml 0.1 M IPTG, which induced CI expression in strain JL5895 and allowed growth of the *lacO*-bearing recombinants in JL2497. Turbid plaques were screened for inability to grow in JL2497 in the absence of IPTG. Presence of *lacO* was verified by DNA sequencing. Plaques are clear on JL6142 or on JL2497 with IPTG, because the *v1* and *v3* mutations in O_R prevent repression of P_R by CI.

λJL481 -- λJL489 was crossed with pJWL631 (5), which is O_R^+, with 0.2 ml 0.1 M IPTG in the top agar. Cross progeny were plated on JL2497 with 0.2 ml 0.1 M IPTG in the top agar; phages forming turbid plaques were isolated. Presence of O_R^+ was verified by DNA sequencing.

λJL483 -- isolated as λJL481, except that cross was with pJWL487 (5), carrying *prm240*.

B.2. Phages with altered O_L regions

Strains JL9114, JL9115 and JL9116 (carrying plasmids with O_L^+, *IHFmut* and *ΔUP*, respectively) were grown in LBMM1 + 1 mM IPTG at 30° C. IPTG induced expression of the thermolabile CI857*ts* repressor from pJWL327, affording repression of P_L on the respective plasmids at 30° C. Cells were grown to 2 x 10^8 / ml, concentrated 10-fold by centrifugation, and infected at low moi with λJL481 or λJL483 for 20 min at room temperature. Cells were diluted into LBGM1 at 40° C; cultures were shaken 90 min and treated with chloroform. Lysates were plated on JL7937, and the resulting P_{RM}^+ $LacI^R$ phage, **λJL1646** *IHFmut* and **λJL1647** *ΔUP*, were characterized as described in Section C below.

Versions carrying *c*I857 were isolated by crossing λJL163 with pJWL326 or by crossing λJL1646 or λJL1647 with pJWL521. Crosses were done at 37° C, followed by plating at 40° C. Large clear plaques were isolated and tested for formation of turbid plaques at 30° C; presence of *c*I857 was verified by sequencing, yielding **λJL1383, λJL1680** and **λJL1682**, respectively.

B.3. Reporter phages carrying P_{RM}::*lacZ* protein fusions

These were made in three steps as described ((5), see Supplemental Material), using one of eight plasmids (see Table S2). Intermediate phages are listed in Table S2; the final constructs are listed in Table S3. The structure of these phages is as shown in (5). Plaque color was assessed by plating with 0.05 ml 2% Xgal in the top agar ("Xgal plates"). First, λJL301 (1) was crossed with cells carrying one of the plasmids indicated in the fourth column; white plaques on Xgal plates were isolated, and the desired recombinants were identified by PCR (1), yielding the

promoter-less reporter phages listed in the fifth column. Presence of the O_L allele was verified by DNA sequencing. Second, these phages were crossed with pJWL479, and recombinants forming dark blue plaques on Xgal plates were isolated, yielding the strains listed in the sixth column. Third, these phages were crossed with pJWL474, pJWL337, pJWL1189 or pJWL1190, which are P_{RM}^+, *prm240*, P_{RM}^+ O_R3 *r1*, or *prm240* O_R3 *r1*, respectively; pale blue or white plaques on Xgal plates were isolated, giving the set of phages listed in Table S3. Presence of the O_R alleles was verified by DNA sequencing in each case. Note that pJWL1189 was also used in this step in the previous study (5), not pJWL488 as was indicated in (5).

C. Pleiotropic effects of *IHFmut* and *ΔUP* mutations on phage physiology

We tested the effects of *IHFmut* and *ΔUP* on several aspects of phage physiology. Both mutations caused mild defects in burst size and lysogenization frequency in the wild-type host in rich medium. The burst sizes of λ wild-type, λ *IHFmut* and λ *ΔUP* after single infection were about 180, 120 and 90, respectively. Lysogenization frequencies after multiple infection were about 70%, 60% and 50%, respectively. λ *prm240 IHFmut* and λ *prm240 ΔUP* were unable to lysogenize, as expected, since they should make less CI than λ *prm240*, for which lysogens are barely stable due to low CI levels (5). They were not further characterized.

Lysogens of λJL1646 *IHFmut* and λJL1647 *ΔUP* produced very low yields upon UV induction (Fig. S3). This defect might result from defects in inactivating CI by specific cleavage. Alternatively, it might result from a defect in expression of one or more functions required for prophage excision, since this is the main aspect of the induction pathway not shared with lytic growth after infection, which was almost normal (see above).

To test whether the induction defect resulted from a failure to inactivate CI by cleavage, we inactivated CI using a temperature-sensitive mutant CI. We made derivatives of these phages carrying the *c*I857*ts* allele (λJL1383, λJL1680 and λJL1682), and carried out thermal induction of lysogens. Again, both mutants had a reduced burst size, yielding about 40 and 25 phage per cell for λ *c*I857 *IHFmut* and λ *c*I857 *ΔUP*, respectively, compared to 150 for the λ *c*I857 lysogen. Although these defects are not as severe as in the case of UV induction, this finding suggests that the defect after UV induction does not result entirely from failure to inactivate CI.

If *IHFmut* or *ΔUP* weaken P_L, levels of Int or Xis proteins may not suffice to support prophage excision. When we provided Int protein *in trans* from a plasmid carrying an IPTG-

inducible *int* gene, the growth defect after prophage induction was partially suppressed (Fig. S4). Provision of Int also partially suppressed the induction defect of *c*I857*ts* derivatives (not shown).

When these mutants were plated at 30° C, they formed small plaques on a *recA*$^+$ host. On a *recA*$^-$ host, plaques were small on tryptone plates; on M9 minimal plates they were tiny and took two days to form. Inability to form plaques on a *recA*$^-$ host (the Fec phenotype (6)) is thought to arise from a defect in the *gam* gene, leading to a requirement for RecA-dependent recombination to generate packageable DNA (7). Perhaps expression of Gam function was defective in the mutants. In any case, this property afforded a selection for variants able to form plaques in one day. Sequencing of the O_L and O_R regions, and the *cro* gene, identified mutations in several loci. These included many in O_L1 and O_L2; in the Shine-Dalgarno sequence of *cro*; a mutation termed *cro-z8* in the *cro* 5'UTR that reduces Cro expression (5); and several mutations in the *cro* gene. The mutations in O_L1 and O_L2 are known from analysis of changes in O_R1 (8) to weaken Cro binding in the context of O_R1. A similar distribution of suppressors was seen for λ *IHFmut* and λ *ΔUP*, suggesting that both mutants are defective in the same process. We surmise that these variants can grow because repression of P_L by Cro is weaker than in the parental phages, allowing increased expression of the *gam* gene.

D. Selection and screen for mutants defective in looping-mediated stimulation

The *prm240* promoter is markedly stimulated by looping between O_L and O_R (5). In addition, lysogens of λ*prm240* are barely stable in rich medium, but more stable in minimal medium. We reasoned that, if looping stimulates P_{RM} through the action of *cis*-acting sites in the O_L region, then lysogens of mutants defective in such sites would be destabilized, and that when such mutants arose the cells would eventually release them as free phage. This approach should identify any relevant *cis*-acting sites, whether or not these had been identified by sequence analysis or genetic analysis. The region between O_L and T_{imm} is highly conserved among a family of wild phages with λ immunity specificity (9), suggesting that other functional sites might lie in this region. To test this prediction, we grew lysogens of strain JL6112 *recA*$^-$ (λ*prm240*) under conditions (M9 minimal medium at 30° C) that yield a very low level of free phage. Typically, at cell densities of 1-2 x 10^8, free phage are present in such cultures at roughly

10^3/ml; destabilizing mutants should be enriched in the free phage population, which could be analyzed in a secondary screen based on plaque phenotype.

λ*prm240* forms turbid plaques indistinguishable from those of WT (5), but we expected that the desired mutants would form plaques less turbid than those of λ*prm240*. In an initial screen, free phage from five independent cultures were plated on JL2497 on tryptone plates at 37° C. A range of plaque morphologies was seen. Sequencing of the O_L region, the O_R region, and part of the *c*I gene showed that isolates forming clear plaques generally had mutations in *c*I. Several isolates forming plaques less turbid than the majority type had a mutation in O_L2. We reasoned that an O_L2 mutant would not be able to support CI-mediated looping. Among many more isolates with the less-turbid plaque phenotype shown by λ*prm240* O_L2^-, nearly all had changes in O_L2. Aside from one isolate with a change that affects P_{RM} and O_R3, we did not identify any mutations in *cis*-acting sites other than the O_L operators.

Two different properties of the *IHFmut* or *ΔUP* mutants would each suffice to make this approach fail. Both the defect in prophage induction (Fig. S4) and formation of very tiny plaques on M9 at 30° C suggest that the burst size of these mutants, should they arise, would be very low, reducing the likelihood of their detection in the "enriched" population of free phage.

E. K_B model – Calculation of relative activity for templates that can loop

We consider the following model for the action of the UP element, simplified from Fig. 8 (Main Text) by omission of parallel forms:

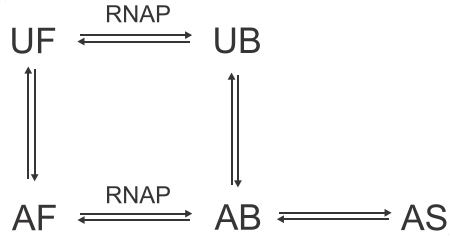

According to the K_B model (see Main Text), the UP element operates by stabilizing AS and driving the equilibrium among these forms towards AS. The goal is to assess the effect of this on the overall activity. Here we calculate the relative activity of the promoter, with and without the presence of the looped forms AF, AB and AS, as a function of three equilibrium constants:

1. K_B, the equilibrium constant between UF and UB
2. X, the equilibrium constant between unlooped and looped forms, related to the value of ΔG_{oct}
3. Y, the equilibrium constant between AB and AS

It is assumed for simplicity that UB, AB and AS all have the same activity.

For the template that cannot loop, the fraction of active templates is

$[UB] / ([UB] + [UF])$ (**1**)

For the template that can loop, the fraction of active templates is

$([UB] + [AB] + [AS]) / ([UB] + [AB] + [AS] + [UF] + [AF])$ (**2**)

We express the concentrations of all species in terms of [UF]:

By definition, where $[RNAP_f]$ is the concentration of free RNAP:

$K_B = [UB] / [RNAP_f] \cdot [UF]$

K_B is an association constant, with units of M^{-1}. Rearranging:

[UB] $= [UF] \cdot (K_B \cdot [RNAP_f])$ (**3**)

[AF] $= X \cdot [UF]$ (**4**)

Where X, the equilibrium constant for this interconversion, is calculated from ΔG_{oct} by

$K_{oct} = \exp(-\Delta G_{oct} / RT)$ where R is the gas constant and T is the temperature

$L = K_{oct} / (1 + K_{oct})$ where L is fraction looped

$X = L / (1 – L)$

$[AB] = [AF] \cdot (K_B \cdot [RNAP_f])$

[AB] $= [UF] \cdot X \cdot (K_B \cdot [RNAP_f])$ (**5**)

$[AS] = Y \cdot [AB]$ where Y is equilibrium constant between AS and AB

[AS] $= [UF] \cdot Y \cdot X \cdot (K_B \cdot [RNAP_f])$ (**6**)

For the looping case, the active fraction is given by (**2**):

$([UB] + [AB] + [AS]) / ([UB] + [AB] + [AS] + [UF] + [AF])$

Active species $([UB] + [AB] + [AS])$ are given by substituting (**3**), (**5**) and (**6**):

$$[UF] \cdot (K_B \cdot [RNAP_f] + X \cdot K_B \cdot [RNAP_f] + X \cdot Y \cdot K_B \cdot [RNAP_f])$$
$$= [UF] \cdot K_B \cdot [RNAP_f] \cdot (1 + X + X \cdot Y)$$

Total species also include UF and AF (from (**4**)):

$$[UF] \cdot K_B \cdot [RNAP_f] \cdot (1 + X + X \cdot Y) + [UF] + [UF] \cdot X$$

After cancelling [UF], the ratio, giving the active fraction of templates, is

$K_B \cdot [RNAP_f] \cdot (1 + X + X \cdot Y) / \{1 + X + K_B \cdot [RNAP_f] \cdot (1 + X + X \cdot Y)\}$ (**7**)

For the unlooped case, the active fraction is given by (**1**):

$[UB] / ([UB] + [UF])$

$= [UF] \cdot (K_B \cdot [RNAP_f]) / \{ [UF] + [UF] \cdot (K_B \cdot [RNAP_f]) \}$

$= (K_B \cdot [RNAP_f]) / (1 + K_B \cdot [RNAP_f])$ (**8**)

The desired result is the ratio Z, which represents the fold stimulation by looping:

Z = activity of the looped template / activity of unlooped template. Canceling terms,

$Z = \langle (1 + X + X \cdot Y) / \{1 + X + K_B \cdot [RNAP_f] \cdot (1 + X + X \cdot Y)\} \rangle / \langle 1 / (1 + K_B \cdot [RNAP_f]) \rangle$

Rearranging,

$Z = \{(1 + X + X \cdot Y) (1 + K_B \cdot [RNAP_f])\} / \{1 + X + K_B \cdot [RNAP_f] \cdot (1 + X + X \cdot Y) \}$ (**9**)

This equation was solved numerically for several values of ΔG_{oct} (which yields X) and a range of Y values, calculating the value in each case of $K_B \cdot [RNAP_f]$ that gave a value of Z of 1.6 (representing the P_{RM}^+ case) or 5 (representing the *prm240* case). See Fig. S5.

F. Possible effects of supercoiling

Although the loop is usually depicted as a simple structure (Figs. 1 and 8, Main Text), in fact the DNA is probably supercoiled much or most of the time. We first discuss the forms taken by supercoiled DNA *in vitro*, and presumably in the cell, then we address the possible consequences for the λ system in light of our findings.

Supercoiled DNA forms a plectonemic superhelix (Fig. 8B left), in which a segment of duplex DNA forms a loop with the two arms intertwined (10). Rapid sliding of the two arms with respect to one another (arrows in figure), juxtaposes a given site on one helix with many sites on the opposite helix, raising their effective local concentration roughly 100-fold relative to that on relaxed DNA (10). This “slithering” should favor octamer formation (Fig. 8B right).

When DNA is transcribed, the moving RNAP follows a helical path around the helix axis (11). If the DNA is free to rotate, it can do so. If the DNA is fixed in a loop, however, it cannot rotate to any extent. In this case, the RNAP can rotate about the DNA, but, due to coupled transcription and translation in prokaryotes, as the mRNA grows it becomes increasingly bulky, and rotation becomes more difficult. More importantly, as RNAP moves, it pushes positive supercoils ahead of itself, and negative supercoils arise in its wake (11, 12). On looped DNA, this would quickly disrupt the superhelix. In addition, the negative supercoils behind the RNAP should facilitate subsequent open complex formation.

Consider now the forms of the DNA segment between λ O_L and O_R. If the DNA is relaxed, the flexibility of DNA allows either the parallel or anti-parallel form. However, if the DNA is in a superhelix prior to CI-mediated loop formation, this should greatly favor the anti-parallel orientation (Fig. 8B right).

When this segment is transcribed, RNAP initiating at P_{RM} transcribes nearly the entire region contained in the loop. If the DNA is unlooped, transcription might affect supercoiling locally, but the supercoils would not affect the overall structure of the segment. If the DNA is looped (Fig. 8B right), transcription will disrupt the superhelix, and we assume for simplicity that such disruption will occur at any time that an RNAP is transcribing the P_{RM} mRNA.

To estimate roughly the fraction of the time this interval is being transcribed, we assume for the moment that transcription is a Poisson process—that is, that the likelihood of an initiation is constant. The transcript is ~2.2 kb long; if RNAP moves at 30 bp/sec, a transcript is made in ~70 sec. The value of k_f on unlooped P_{RM} *in vitro* is 0.012/sec (13); once formed, open complexes generally initiate promptly. We assume for the sake of discussion that CI-mediated looping does not alter k_f (as in the K_B model). Upon initiation, transcription lasts for the next 70 sec. We can set a lower limit on the probability that no initiation will occur in this 70-sec interval by assuming that the promoter is nearly always occupied by RNAP, an assumption compatible with the K_B model, which posits that looping favors RNAP binding (see Main Text). In this case, the probability that no initiation will occur in the next sec is $1 - k_f = 0.988$, and the probability that another initiation will not occur during synthesis of a transcript is 0.988^{70} or ~0.4. This value represents the probability that the region will become non-transcribing when a newly-initiated transcript terminates. It is also the probability that on a non-transcribing template the region will remain non-transcribing for the next 70 sec. If the promoter is free of RNAP a substantial fraction of time, this probability would be larger. In any case, it is plausible that the region exists both in transcribed and non-transcribed states a substantial fraction of the time.

Recent *in vivo* data, including some with a form of P_{RM} that can loop, indicate that initiation is not in fact a Poisson process. Instead, transcription occurs in "bursts" (14, 15); periods of active transcription are interspersed with long periods in which no transcription occurs. For P_{RM}, the burst size is ~4 transcripts. Accordingly, the fraction of time the interval is not being transcribed is larger than the above calculation indicates.

We now relate these considerations to the present findings. First, supercoiling favors the anti-parallel form (Fig. 8B right). However, when the DNA is being transcribed, if the loop breaks and reforms, the anti-parallel form should be much less favored, since the superhelix is disrupted by transcription. If loops form and break rapidly, this might lead to a sizable percentage of the loops in parallel orientation, perhaps as much as 50%. This predicts that, if the O_L region were placed upstream of P_{RM}, so that transcription would not disrupt the superhelix, the anti-parallel form would continue to be favored. In contrast, Cui *et al.* (16) found that the degree of stimulation was the same regardless of the orientation of the O_L region, suggesting either that both parallel and anti-parallel forms are stimulated about equally, and/or that both forms are about equally probable on their templates.

Second, if the promoter is weaker, as with *prm240*, the fraction of time that the interval is supercoiled increases, further favoring the anti-parallel conformation. This suggests one mechanism by which *prm240* could be stimulated by looping to a greater extent than P_{RM}^{+}, although it is probably not the only mechanism (see Main Text).

Third, there are two IHF binding sites in the O_L region (17-19). In addition to the site studied here, a second, less well-defined site (termed L2) lies close to the T_{imm} terminator. Bends created by IHF might affect the relative probability of the two looped orientations of O_L and O_R; for simplicity we suggest that the two bends offset one another, with the net effect that the anti-parallel orientation of the O_L region is preferred. If so, then blocking binding of IHF to the L1 site would disfavor the anti-parallel conformation, leading to a loss of stimulation. Such an effect would be more severe for *prm240*, if, the mutant template is supercoiled a greater fraction of the time. This fits with the lack of stimulation in the *IHFmut prm240* case (Fig. 3C and 3D). In contrast, the wild-type would be less affected, as observed (Fig. 3A and 3B).

Fourth, because of the creation of negative supercoils behind the advancing RNAP, transcription would favor open complex formation by the next RNAP. This would offer a simple mechanism for bursting, if supercoils do not relax before subsequent initiations occur, as suggested (20). This effect would be greater in a looped complex, because relaxation of negative supercoils would be much slower, and might contribute to the bursting seen with P_{RM} (14, 15).

Evaluating the impact of supercoiling is made still more difficult by other uncertainties regarding CI-mediated looping. The rates at which the loop forms and dissociates are unknown.

Can a loop persist through several transcription events? Does the αCTD-UP element interaction make an anti-parallel loop last longer? Conversely, might transcription initiation destabilize the loop by putting torque on the DNA?

References Cited

1. **Michalowski CB, Short MD, Little JW.** 2004. Sequence tolerance of the phage λ P_{RM} promoter: Implications for evolution of gene regulatory circuitry. J. Bacteriol. **186:**7988-7999.
2. **Atsumi S, Little JW.** 2004. Regulatory circuit design and evolution using phage λ. Genes Dev. **18:**2086-2094.
3. **Sanger F, Coulson AR, Hong GF, Hill DF, Petersen GB.** 1982. Nucleotide sequence of bacteriophage λ DNA. J.Mol.Biol. **162:**729-773.
4. **Giese KC, Michalowski CB, Little JW.** 2008. RecA-dependent cleavage of LexA dimers. J Mol.Biol. **377:**148-161.
5. **Little JW, Michalowski CB.** 2010. Stability and instability in the lysogenic state of phage lambda. J. Bacteriol. **192:**6064-6076.
6. **Zissler J, Signer E, Schaefer F.** 1971. The role of recombination in growth of bacteriophage lambda I. The gamma gene, p. 455-468. *In* Hershey AD (ed.), The Bacteriophage Lambda. Cold Spring Harbor Laboratory.
7. **Enquist LW, Skalka A.** 1973. Replication of bacteriophage λ DNA dependent on the function of host and viral genes I. Interaction of *red, gam* and *rec*. J.Mol.Biol. **75:**185-212.
8. **Takeda Y, Sarai A, Rivera VM.** 1989. Analysis of the sequence-specific interactions between Cro repressor and operator DNA by systematic base substitution experiments. Proc.Natl.Acad.Sci.U.S.A. **86:**439-443.
9. **Degnan PH, Michalowski CB, Babić AC, Cordes MHJ, Little JW.** 2007. Conservation and diversity in the immunity regions of wild phages with the immunity specificity of phage λ. Mol. Microbiol. **64:**232-244.
10. **Vologodskii AV, Levene SD, Klenin KV, Frank-Kamenetskii M, Cozzarelli NR.** 1992. Conformational and thermodynamic properties of supercoiled DNA. J.Mol.Biol. **227:**1224-1243.
11. **Liu LF, Wang JC.** 1987. Supercoiling of the DNA template during transcription. Proc.Natl.Acad.Sci.U.S.A. **84:**7024-7027.
12. **Wu HY, Shyy S, Wang JC, Liu LF.** 1988. Transcription generates positively and negatively supercoiled domains in the template. Cell **53:**433-440.
13. **Shih MC, Gussin GN.** 1983. Mutations affecting two different steps in transcription initiation at the phage λ P_{RM} promoter. Proc.Natl.Acad.Sci.U.S.A. **80:**496-500.

14. **Golding I, Paulsson J, Zawilski SM, Cox EC.** 2005. Real-time kinetics of gene activity in individual bacteria. Cell **123:**1025-1036.
15. **So L, Ghosh A, Zong C, Sepúlveda LA, Segev R, Golding I.** 2011. General properties of transcriptional time series in *Escherichia coli* Nat.Genet. **43:**554-560.
16. **Cui L, Murchland I, Shearwin KE, Dodd IB.** 2013. Enhancer-like long-range transcriptional activation by λ CI-mediated DNA looping. Proc.Natl.Acad.Sci.U.S.A **110:**2922-2927.
17. **Giladi H, Koby S, Prag G, Engelhorn M, Geiselmann J, Oppenheim AB.** 1998. Participation of IHF and a distant UP element in the stimulation of the phage λ P_L promoter. Mol. Microbiol. **30:**443-451.
18. **Giladi H, Murakami K, Ishihama A, Oppenheim AB.** 1996. Identification of an UP element within the IHF binding site at the P_L1-P_L2 tandem promoter of bacteriophage λ. J.Mol.Biol. **260:**484-491.
19. **Giladi H, Gottesman M, Oppenheim AB.** 1990. Integration host factor stimulates the phage lambda pL promoter. J.Mol.Biol. **213:**109-121.
20. **Mitarai N, Dodd IB, Crooks MT, Sneppen K.** 2008. The generation of promoter-mediated transcriptional noise in bacteria. PLoS.Comput.Biol. **4:**e1000109.
21. **Little JW.** 1984. Autodigestion of lexA and phage lambda repressors. Proc.Natl.Acad.Sci.U.S.A. **81:**1375-1379.
22. **Little JW, Shepley DP, Wert DW.** 1999. Robustness of a gene regulatory circuit. EMBO J. **18:**4299-4307.
23. **Atsumi S, Little JW.** 2006. Role of the lytic repressor in prophage induction of phage λ as analyzed by a module-replacement approach. Proc.Natl.Acad.Sci.U.S.A. **103:**4558-4563.
24. **Simons RW, Houman F, Kleckner N.** 1987. Improved single and multicopy *lac*-based cloning vectors for protein and operon fusions. Gene **53:**85-96.
25. **Mustard JA, Little JW.** 2000. Analysis of *Escherichia coli* RecA interactions with LexA, lambda CI, and UmuD by site-directed mutagenesis of *recA*. J. Bacteriol. **182:**1659-1670.
26. **Krause M, Rückert B, Lurz R, Messer W.** 1997. Complexes at the replication origin of *Bacillus subtilis* with homologous and heterologous DnaA protein. J.Mol.Biol. **274:**365-380.
27. **Whipple FW, Kuldell NH, Cheatham LA, Hochschild A.** 1994. Specificity determinants for the interaction of λ repressor and P22 repressor dimers. Genes Dev. **8:**1212-1223.
28. **Little JW, Hill SA.** 1985. Deletions within a hinge region of a specific DNA-binding protein. Proc.Natl.Acad.Sci.U.S.A. **82:**2301-2305.
29. **Lin LL, Little JW.** 1989. Autodigestion and RecA-dependent cleavage of Ind^- mutant LexA proteins. J.Mol.Biol. **210:**439-452.
30. **Beamer LJ, Pabo CO.** 1992. Refined 1.8 Å crystal structure of the λ repressor-operator complex. J.Mol.Biol. **227:**177-196.
31. **Rice PA, Yang SW, Mizuuchi K, Nash HA.** 1996. Crystal structure of an IHF-DNA complex: A protein-induced DNA U-turn. Cell **87:**1295-1306.
32. **Sayle R, Milner-White EJ.** 1995. RasMol: Biomolecular graphics for all. Trends in Biochemical Sciences **20:**374-374.

TABLE S1. BACTERIAL, PHAGE AND PLASMID STRAINS

Strain	Relevant genotype	Source or reference
a. Bacterial strains[a]		
JL468	AB1157 / F'*lacI*^{q}	(21)
JL5242	Derivative of JL2497 with F' *lacI*^{q}*lacZ*ΔM15::Tn*3* replacing F' *lacI*^{q}*lacZ*ΔM15::Tn*9*	(2)[b]
JL5292	JL468 / pA3B2	This work
JL5830	JL468 / pJWL326	
JL5832	JL468 / pJWL327	This work
JL5895	JL5242 / pA3B2	(2)
JL5932	JL2497 (λJL163)	(22)
JL6112	JL5902(λJL240)	(5)
JL6142	JL2497 Δ(*lacIPOZYA*) F^{-}	(2)
JL7022	JL468/pJWL521	This work
JL7209	JL5292 / pJWL808	This work
JL7937	JL6142 / pJWL614	This work
JL8524	JL2497 (λJL1383)	This work
JL9058	DH5α / pJAM13	This work
JL9114	JL5832 / pJWL1293	This work
JL9115	JL5832 / pJWL1294	This work
JL9116	JL5832 / pJWL1295	This work
JL9121	JL2497 (λJL1646)	This work
JL9311	JL2497 (λJL1680)	This work
JL9314	JL2497 (λJL1682)	This work
JL9341	JL2497 (λJL1647)	This work
DH5α	Δ(*lacZYA-argF*)U169 *recA1 endA1 hsdR17*(r_K^- m_K^+) *phoA supE44 thi-1 gyrA96 relA1* (ϕ80 *lacZΔM15*). Used for high-efficiency transformation of SDM ligation mixtures.	Invitrogen

b. Phage strains[c]			
λJL163	λ *bor::kan* , used as wild-type λ ; remaining λ strains are derivatives of this strain [a]		(22)
λJL240	λ *prm240*		(5)
λJL481	λ *lacO* / P_L O_R^+		This work
λJL483	λ *lacO* / P_L *prm240*		This work
λJL489	λ *lacO* / P_L *v1 v3*		This work
λJL537	λ *v2 v1 v3*		(5)
λJL1646	λ *IHFmut*		This work
λJL1647	λ *ΔUP*		This work
λJL1383	λ *cI857ts*		This work
λJL1680	λ*cI857ts IHFmut*		This work
λJL1682	λ *cI857ts ΔUP*		This work
	c. Plasmids	Vector	
pJWL326	Derivative of pLR1 with *lacP*::*cI857ts*	pBR322	This work
pJWL327	Derivative of pA3B2 with *lacP*::*cI857ts*	pACYC184	This work
pJWL334	Derivative of pBS(-) with modified polylinker. Amp^R; high copy-number	pBS(-)	(1)
pJWL487	Derivative of pJWL334; carries λ O_R region with *prm240* allele	pBS(-)	(5)
pJWL521	Derivative of pBR322 with truncated *c*I857 gene	pBR322	This work
pJWL614	$lacI^q$ Amp^R ; medium copy-number	pBR322	(23)
pJWL611	Derivative of pRS308 lacking *lacA* and most of *lacY*, with multiple cloning site and *trp a* located distal to the end of *lacZ*	pBR322	(24); (1)
pJWL631	Derivative of pJWL334; carries wild-type λ O_R region	pBS(-)	(5)
pJWL808	Derivative of pJWL334; carries λ O_L region with *lacO* at P_L (see Text)	pBS(-)	(2)
pJWL1157	λ O_L region cloned into pJWL611	pBR322	(5)
pJWL1158	O_L3-4 derivative of pJWL1157	pBR322	(5)
pJWL1293	Derivative of pJWL334; carries λ O_L region	pBS(-)	This work
pJWL1294	Derivative of pJWL334; carries λ O_L region with	pBS(-)	This work

	IHFmut		
pJWL1295	Derivative of pJWL334; carries λ O_L region with *ΔUP*	pBS(-)	This work
pJAM13	lacP::*c*I	pGB2	(25)
pLEXInt	Carries *lacI* and λ *int* gene fused to the IPTG-inducible $P_{A1-O3/O4}$ promoter in pLEX5BA	pBR322	Anca Segall
pLEX5BA	Cloning vector; carries *lacI* and multiple cloning site downstream of IPTG-inducible, tightly-regulated $P_{A1-O3/O4}$ promoter	pBR322	Anca Segall; (26)
pLR1	Carries a weak *lacP*::*c*I fusion	pBR322	(27)

[a] Not listed are derivatives of JL5932, JL8524, JL9121, JL9341, JL9311, and JL9314 carrying pLEXInt or the control plasmid pLEX5BA.

[b] F' *lacI*^{q}*lacZ*ΔM15::Tn*3* was transferred from JL795 (28) to JL853 (29) with selection for Amp^R and *tonA*, then to JL2497 with selection for Amp^R and Str^R. Used but not named in (2).

[c] All λ strains listed carry the *bor::kan* allele

Table S2. Intermediates for construction of P_{RM}::*lacZ* protein fusions

O_L allele	Template for SDM	Primers for SDM	Resulting plasmid	Promoterless phage	P_R::*lacZ* fusion
ΔUP	pJWL1157	105for, 85rev	pJWL1279	λJL1610	λJL1620
ΔUP O_L3-4	pJWL1279	oL3mutf, oL3rev	pJWL1297	λJL1644	λJL1651
IHFmut	pJWL1157	80for, 79mutrev	pJWL1278	λJL1609	λJL1619
IHFmut O_L3-4	pJWL1278	oL3IHF2X, oL3rev	pJWL1296	λJL1643	λJL1650
Δ(70-102)	pJWL1157	IHF102for, IHF70rev	pJWL1241	λJL1530	λJL1559
Δ(70-102) O_L3-4	pJWL1158	IHF102for, ol3mut70rev	pJWL1267	λJL1551	λJL1565
O_L1-3	pJWL1157	oL1for, oL1mutrev	pJWL1280	λJL1611	λJL1621
O_L1-3 O_L3-4	pJWL1280	oL3mutf, oL3rev	pJWL1298	λJL1645	λJL1652

Table S3 – phages carrying P_{RM}::*lacZ* protein fusions with various O_L alleles distal to *lacZ*

Phage strain name	O_L allele	P_{RM} allele	Source or reference
λJL1366	T_{imm}	P_{RM}^+	(5)
λJL1367	O_L^+	P_{RM}^+	(5)
λJL1370	O_L3-4	P_{RM}^+	(5)
λJL1626	*ΔUP*	P_{RM}^+	This work
λJL1654	*ΔUP* O_L3-4	P_{RM}^+	This work
λJL1625	*IHFmut*	P_{RM}^+	This work
λJL1653	*IHFmut* O_L3-4	P_{RM}^+	This work
λJL1578	Δ(70-102)	P_{RM}^+	This work
λJL1584	Δ(70-102) O_L3-4	P_{RM}^+	This work
λJL1627	O_L1-3	P_{RM}^+	This work
λJL1655	O_L1-3 O_L3-4	P_{RM}^+	This work
λJL1394	T_{imm}	P_{RM}^+ O_R3-*r1*	(5)
λJL1395	O_L^+	P_{RM}^+ O_R3-*r1*	(5)
λJL1396	O_L3-4	P_{RM}^+ O_R3-*r1*	(5)
λJL1660	*ΔUP* O_L3-4	P_{RM}^+ O_R3-*r1*	This work
λJL1703	*IHFmut*	P_{RM}^+ O_R3-*r1*	This work
λJL1659	*IHFmut* O_L3-4	P_{RM}^+ O_R3-*r1*	This work
λJL1675	Δ(70-102) O_L3-4	P_{RM}^+ O_R3-*r1*	This work
λJL1674	O_L1-3	P_{RM}^+ O_R3-*r1*	This work
λJL1661	O_L1-3 O_L3-4	P_{RM}^+ O_R3-*r1*	This work
λJL1375	T_{imm}	*prm240*	(5)
λJL1376	O_L^+	*prm240*	(5)
λJL1377	O_L3-4	*prm240*	(5)
λJL1632	*ΔUP*	*prm240*	This work
λJL1657	*ΔUP* O_L3-4	*prm240*	This work
λJL1631	*IHFmut*	*prm240*	This work
λJL1656	*IHFmut* O_L3-4	*prm240*	This work
λJL1633	O_L1-3	*prm240*	This work
λJL1658	O_L1-3 O_L3-4	*prm240*	This work
λJL1585	Δ(70-102)	*prm240*	This work
λJL1591	Δ(70-102) O_L3-4	*prm240*	This work
λJL1391	T_{imm}	*prm240* O_R3-*r1*	(5)
λJL1392	O_L^+	*prm240* O_R3-*r1*	(5)
λJL1393	O_L3-4	*prm240* O_R3-*r1*	(5)
λJL1663	*ΔUP* O_L3-4	*prm240* O_R3-*r1*	This work
λJL1662	*IHFmut* O_L3-4	*prm240* O_R3-*r1*	This work
λJL1678	Δ(70-102) O_L3-4	*prm240* O_R3-*r1*	This work
λJL1677	O_L1-3	*prm240* O_R3-*r1*	This work
λJL1664	O_L1-3 O_L3-4	*prm240* O_R3-*r1*	This work

Table S4. Synthetic oligonucleotides used

Name	Sequence
IHF102for	GCAGGGGGGCATTGTTTG
IHF70rev	TAACCATCTGCGGTGATAAATT
ol3mut70rev	TAACCAACTCTAGTGATAAATTAT
IHF80for	TTTTTATATGAATTTATTTTTTGCAG
79mutrev	ACGTACAAACAACCATCTGCGGTG
105for	GGGGGGCATTGTTTGGTA
85rev	TAAAAAACATACAGATAACCATCTG
ol1mutfor	TGATACTGAGCACATCAGCAG
ol1mutrev	ACTCCATTGGTATTTATGTCAACAC
ol3IHF2X	CACTAGAGTTGGTTGTTTGTACG
ol3mutf	CACTAGAGTTGGTTATCTGTATG
ol3rev	ATAAATTATCTCTGGCGGTGTTG
olKpn	CACGGTACCATCTGGATTCTCCTG 35357
bamrexB	GATGGATCCTGCATCCTTGTTTTCCAAC 35872

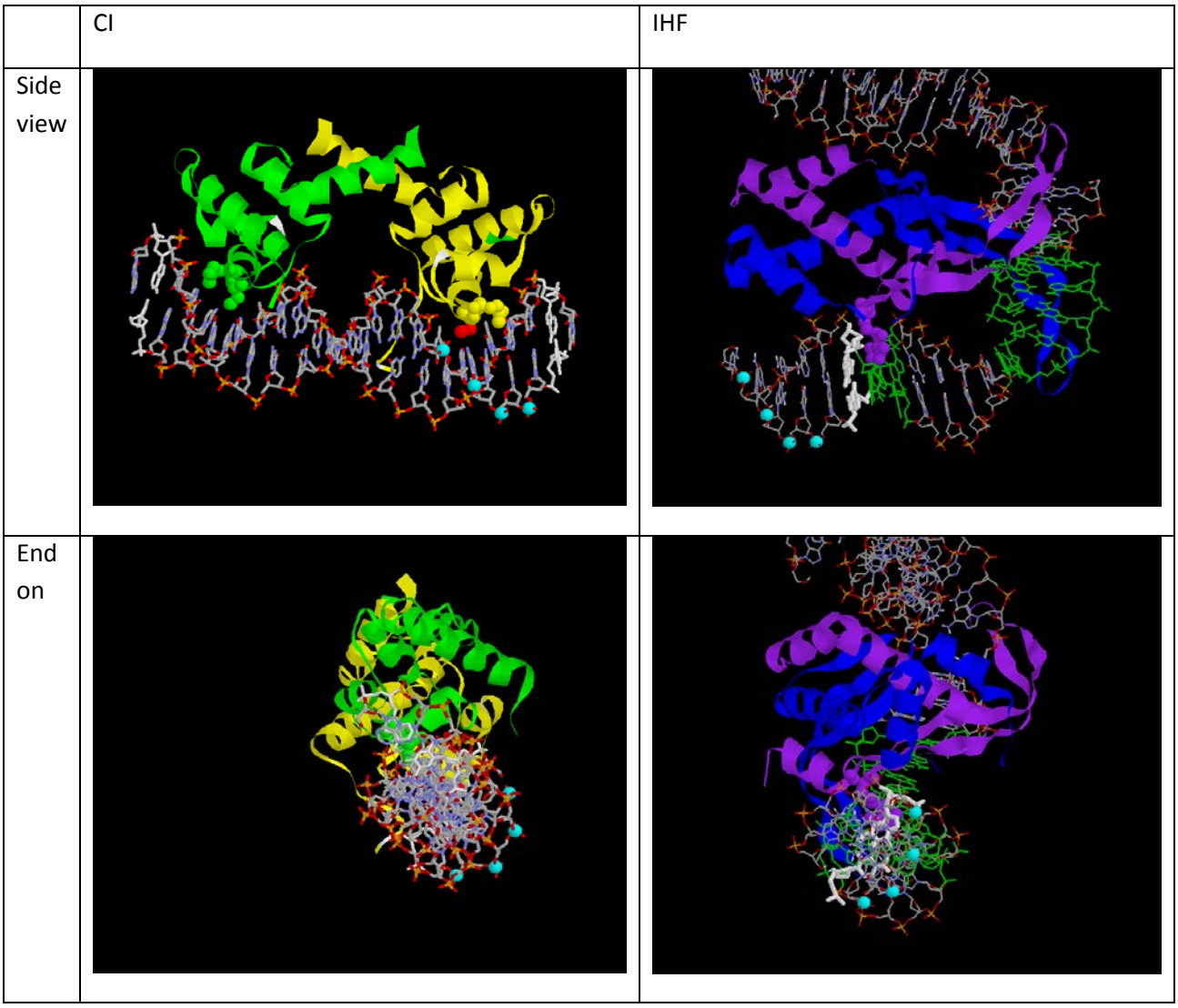

Fig. S1. Clash between IHF and CI bound to O_L3. Shown at left are structures of the CI N-terminal domain bound to O_L1 (30) (1LMB.pdb); figures on the right show IHF bound to a specific site (31) (1IHF.pdb). In the CI structure, the two subunits are shown in green and yellow. In the side view (top left), if the specific binding site were O_L3, the IHF site would lie just to the right, and the white bp would correspond to bp -70. In the IHF structure (top right), the α and β subunits are in blue and purple, respectively. Bases in green or white are the IHF binding site consensus, which which IHF makes specific contacts. O_L3 would lie to the left, and the white bp corresponds to bp -70. This view is similar to that shown in (17). In each structure, the four phosphates in cyan are the same phosphates and are meant to help align the two structures visually. In each, the white base pair at bp -70 is an important IHF contact, which is changed in the *IHFmut* allele. The structures in the top panels are rotated 90° about the y axis to yield those in the bottom panels; taken together the figures indicate that the positions of the two proteins overlap, even in the absence of the CTD of CI, and they could not bind simultaneously to the DNA (see Fig. 6 in Main Text). Figures were generated using RasMol (32).

Figure S2. Phage-by-plasmid crosses to place O_L alleles on phage

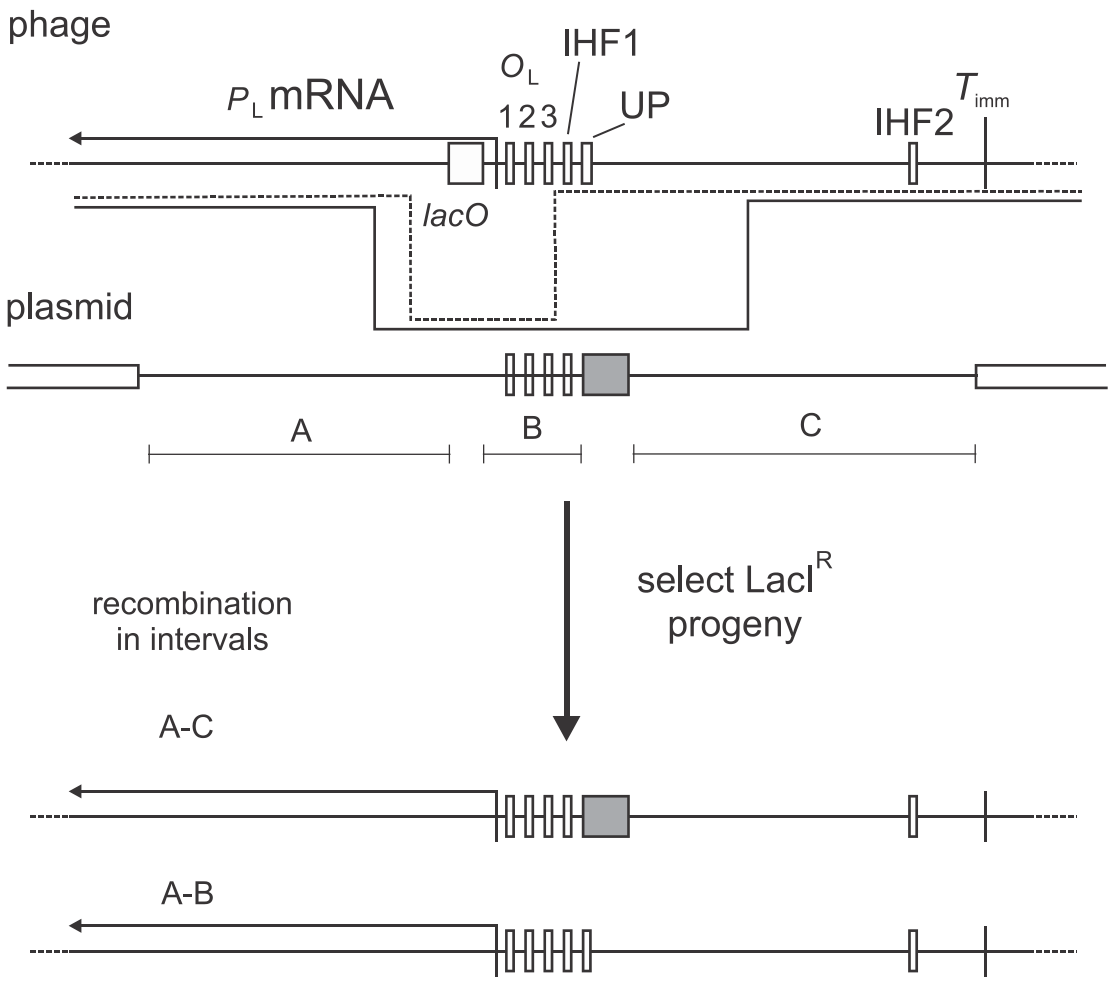

Recombination is between a *lacO* / P_L phage at the top and a plasmid bearing an allele of the O_L region, symbolized by a gray box. *lacO* is symbolized in the phage by the open box. LacI^R recombinants are generated by a first crossover in the interval marked "A"; the second crossover could occur in interval B (dashed line) or C (solid line), yielding the wild-type, recombinant A-B, or the desired recombinant A-C. These can be distinguished either by DNA sequencing of PCR products or (as in the present work), by their altered phenotype.

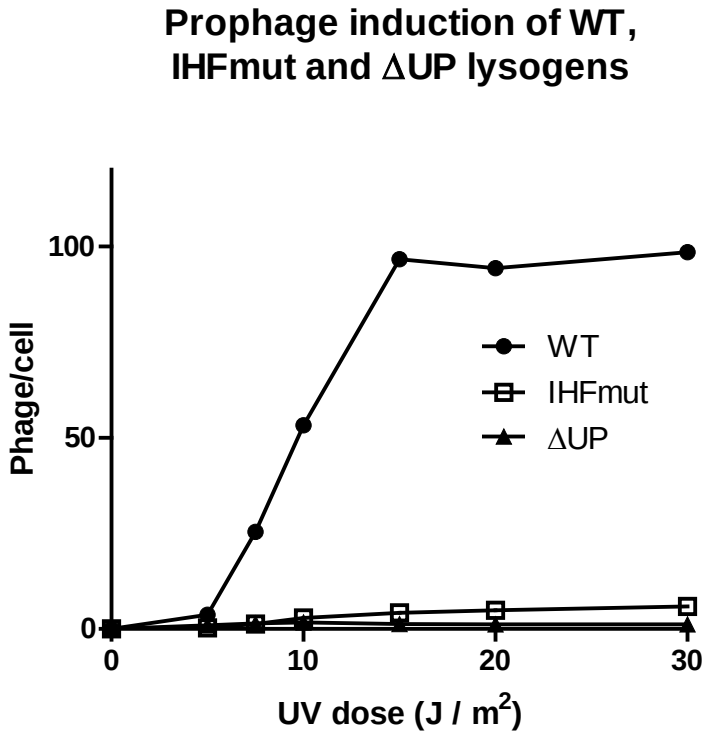

Figure S5

Fig. S3: **Prophage induction defect of λ *IHFmut* and λ *ΔUP***. Prophage induction was carried out as described in Materials and Methods. Lysogens of λJL163, λJL1646 *IHFmut* and λJL1647 *ΔUP* were irradiated with various doses of UV light, and the yield of phage was measured.

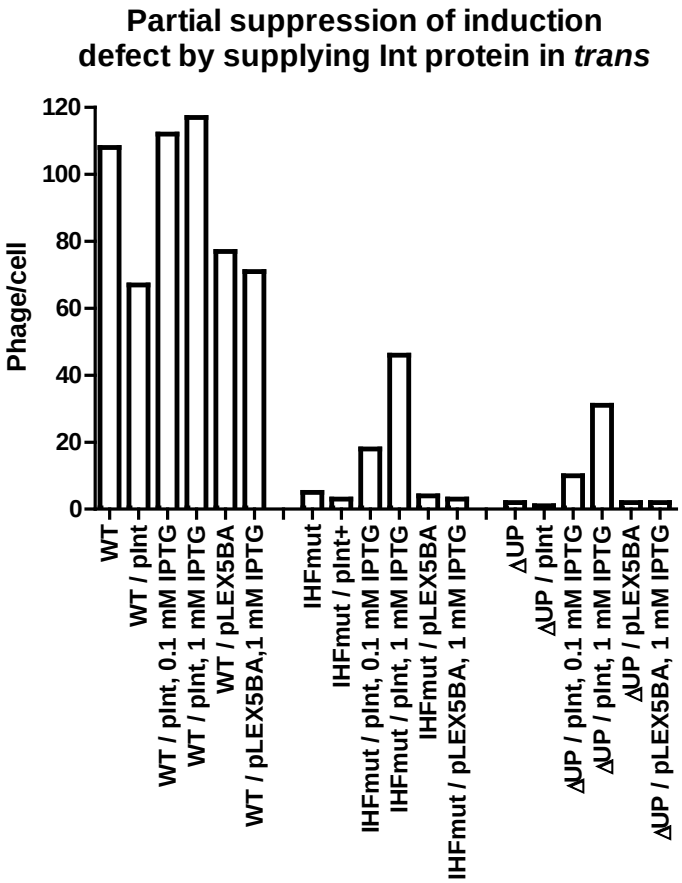

Figure S6

Fig. S4: Partial suppression of induction defects of λ *IHFmut* and λ *ΔUP* by Int protein. The strains used in Fig S3 were transformed either with pLEXInt, which supplies Int under control of an IPTG-inducible promoter, or the pLEX5BA vector used to make pLEXInt as a control. Untransformed controls were also included. Cells were grown and UV-irradiated (20 J/m^2) as described (22). After irradiation, aliquots were diluted 10-fold into medium containing 0, 0.1 or 1 mM IPTG and shaken 2 hr 37° C. Suppression is optimal when pInt is induced by 1 mM IPTG.

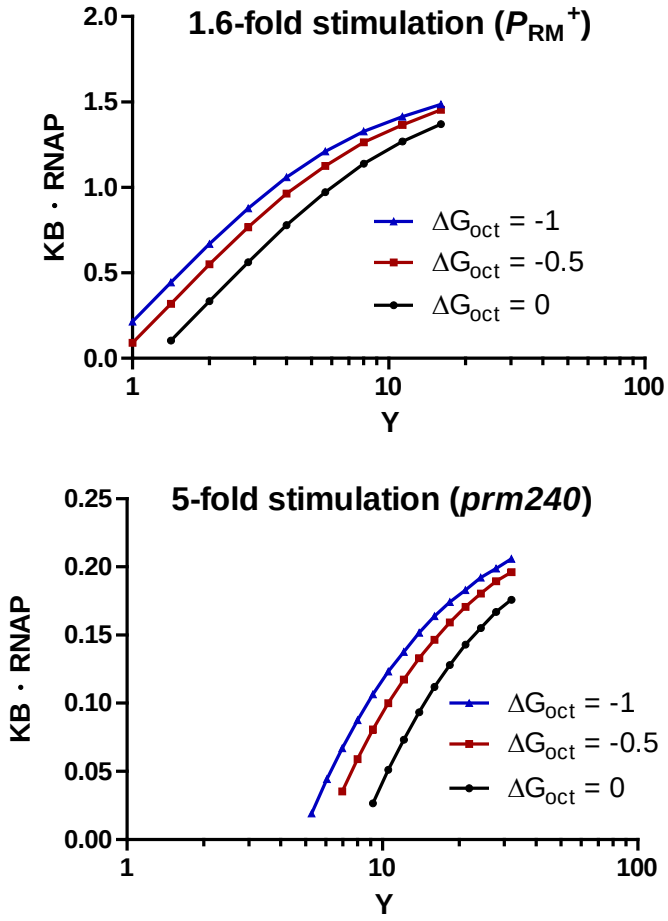

Fig.S5: Analysis of K_B model. For three values of ΔG_{oct} and a range of Y values, equation (**9**) was solved for various values of $K_B \cdot [RNAP_f]$, and the values giving Z values (relative activation due to looping) of 1.6 or 5 were tabulated and plotted. These Z values correspond respectively to the maximal value of looping-mediated activation observed (Fig. 3) for P_{RM}^+ and *prm240*. At low values of $K_B \cdot [RNAP_f]$, RNAP occupies the promoter in a closed complex only a small fraction of the time. For instance, values of 0.1, 0.3 and 1.0 correspond to 9%, 23% and 50% occupancy, respectively. K_B is believed to be substantially lower for *prm240* than for P_{RM}^+ (see Main Text). It is plausible that the value of Y (= [AS]/[AB]) differs for the two promoters, since the value may depend on the details of the conformation in the looped complex.